

Microstructure and dielectric properties control of $\text{Ba}_4(\text{Nd}_{0.7}\text{Sm}_{0.3})_{9.33}\text{Ti}_{18}\text{O}_{54}$ microwave ceramics

Jing Pei, Zhenxing Yue^{*}, Fei Zhao, Zhilun Gui, Longtu Li

*State Key Laboratory of New Ceramics and Fine Processing, Department of Materials Science and Engineering,
Tsinghua University, Beijing 100084, PR China*

Received 10 July 2007; received in revised form 15 August 2007; accepted 6 October 2007

Available online 15 December 2007

Abstract

Microwave ceramics of $\text{Ba}_4(\text{Nd}_{0.7}\text{Sm}_{0.3})_{9.33}\text{Ti}_{18}\text{O}_{54}$ with 0–3 wt% Ag additions were synthesized by a citrate sol–gel method. The $\text{BaO-B}_2\text{O}_3\text{-SiO}_2$ glass was also added into the sol–gel derived BNST ceramic powders as sintering aids. The undoped, Ag- and BaBS-doped samples can be sintered at 1250 °C, 1150 °C and 1000 °C, respectively. The microstructure and dielectric properties were then controlled by doping Ag or BaBS glass. Near isoaxial grains with about 250 nm and typical columnar grains were obtained for the silver-doped and BaBS-doped samples, respectively. For the <1 wt% silver-doped samples, the dielectric constant and $Q \times f$ retained unaltered but τ_f decreased from 9 ppm/°C to 1.4 ppm/°C. With increasing silver content from 1 wt% to 3 wt%, the dielectric constant and τ_f significantly increased but $Q \times f$ decreased. For the BaBS-doped samples, both dielectric constant and $Q \times f$ decreased but τ_f increased with increasing BaBS content.

© 2007 Elsevier Ltd and Techna Group S.r.l. All rights reserved.

Keywords: Ceramics; Dielectrics; Microstructure; Low-temperature sintering

1. Introduction

With the recent progress of microwave integrated circuits, low dielectric loss materials with a high dielectric constant and a near-zero temperature coefficient of resonant frequency have been increasingly required for commercial microwave applications [1]. In particular, with the miniaturization and integration of electronic circuits, small-scale microwave devices are increasingly required. Therefore, the dielectric ceramics with submicron- or nano-sized grains and relatively low sintering temperature are required for the micro-chip microwave capacitors and multilayer dielectric filters. The investigation of lowering sintering temperature has been extensively carried out by many researchers. However, there are few reports, to our knowledge, concerning about the microstructure control for microwave dielectric ceramics. Therefore, controlling the microstructure, such as grain size, in order to cope with thinning the layer thickness is still a challenge.

The tungstenbronze-type like $\text{Ba}_{6-3x}\text{Ln}_{8+2x}\text{Ti}_{18}\text{O}_{54}$ solid solutions have been extensively studied because of their suitability for microwave applications [2–6]. The dielectric characteristics of these solid solutions are sensitive to both the value of x and the identity of the rare-earth ions. The most attractive microwave dielectric properties of high ϵ_r (80–84), high $Q \times f$ value (9000–10,000 GHz), and near-zero τ_f were obtained in Nd- or La-substituted $\text{Ba}_{6-3x}\text{Sm}_{8+2x}\text{Ti}_{18}\text{O}_{54}$ ($x = 0.6, 0.67$ and 0.75) solid solution [7]. However, the high sintering temperature, usually above 1350 °C [6,8], limited the extension of practical applications. Some attempts had been carried out to lower the sintering temperature by adding low melting point oxides or glass compositions with low softening temperature. Unfortunately, by those ways it is difficult to lower the sintering temperature and control microstructure as well as microwave properties simultaneously. Besides, recent reports revealed that the microwave properties were also controlled by grain orientation in $\text{Ba}_{6-3x}\text{Sm}_{8+2x}\text{Ti}_{18}\text{O}_{54}$ ceramics [9]. Accordingly, the microstructure of the sintered $\text{Ba}_{6-3x}\text{Sm}_{8+2x}\text{Ti}_{18}\text{O}_{54}$ ceramics might also affect their microwave dielectric properties, but few were reported.

In this paper, we prepared the modified $\text{Ba}_4(\text{Nd}_{0.7}\text{Sm}_{0.3})_{9.33}\text{Ti}_{18}\text{O}_{54}$ ceramics by a citrate sol–gel method. Ultrafine-grain

^{*} Corresponding author. Tel.: +86 10 62784579; fax: +86 10 62771160.

E-mail address: yuezx@tsinghua.edu.cn (Z. Yue).

BNST ceramics with fine microwave dielectric properties were obtained by silver metal additions. As a comparison, we also modified the BNST ceramics with BaO–B₂O₃–SiO₂ glass (BaBS). The microstructure as well as sintering temperature of the sintered ceramics was successfully tuned by such additives with different characteristics. The effect of these two kinds of dopants on the sintering behavior, microstructure and microwave dielectric properties of the BNST ceramics was systematically discussed.

2. Experimental procedures

Samples of Ba₄(Nd_{0.7}Sm_{0.3})_{9.33}Ti₁₈O₅₄ + *y* Ag (*y* = 0–5 wt.%) were prepared from high-purity Ba(CH₃COOH)₂, Nd(CH₃COOH)₃, Sm(CH₃COOH)₃, Ti(OC₄H₉)₄, and Ag₂O, using a citrate sol–gel method. An appropriate amounts of acetate and citric acid were dissolved into deionized water; Ag₂O was dissolved into nitric acid beforehand, and butyl titanate was dissolved in citric acid solution. These solutions were then mixed together and a small amount of aqueous ammonia was added to adjust pH value to about 6. During this process, the solution was continuously stirred using a magnetic agitator at 80 °C. The mixed solution was then heated at 110 °C and a black foam-like xerogel was obtained. The xerogels were calcined in the temperature range of 700–900 °C for 4 h. For the BaO–B₂O₃–SiO₂ (BaBS)-doped samples preparation, the BaBS powder was added into the calcined undoped Ba₄(Nd_{0.7}Sm_{0.3})_{9.33}Ti₁₈O₅₄ powder at this step. The calcined powders were milled by planetary milling for 5 h in alcohol medium. After drying, the powders were pressed into disk-shaped compacts using uniaxial pressure of 2.5 tonnes/cm². The samples were sintered at 950–1250 °C for 4 h in air.

The bulk densities of the sintered samples were measured by the Archimedes method. The theoretical densities (TD) of these samples were calculated from the theoretical densities of Ba₄Sm_{9.33}Ti₁₈O₅₄ (5.91 g/cm³), Ag (10.50 g/cm³) and BaBS (2.75 g/cm³) according to the nominal silver content. The deviation from the “real” theoretical density of Ba₄(Nd_{0.7}Sm_{0.3})_{9.33}Ti₁₈O₅₄, is small enough to be ignored due to their similar molecular weight and unit-cell volume. The crystalline phases were determined by using an X-ray diffractometer (D/max-2500, Rigaku, Tokyo, Japan) with Cu Kα radiation. The microstructures of sintered samples and powders were observed by scanning electron microscopy (SEM) and transmission electron microscopy (TEM). The

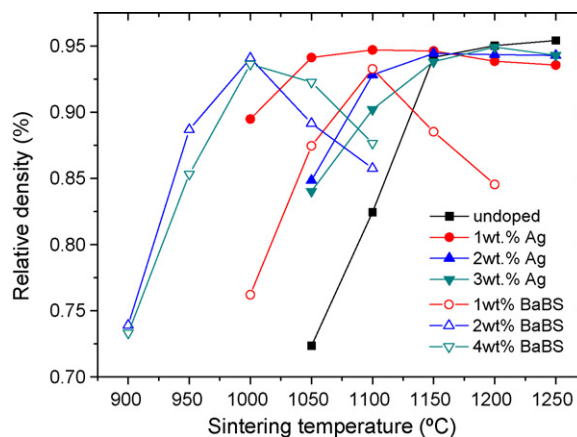


Fig. 1. Relative density variation of the undoped, Ag-doped, and BaBS-doped BNST ceramics with sintering temperatures.

dielectric constants and unloaded *Q* values at microwave frequencies were characterized at room temperature by the Hakki–Coleman method and cavity method [10,11]. The temperature coefficients (τ_f) of the resonance frequencies were measured in the temperature range of 25–80 °C. The τ_f value can be calculated by the following relationship [12]:

$$\tau_f = \frac{f_2 - f_1}{f_1(T_2 - T_1)}$$

where f_1 and f_2 represent the resonant frequencies at T_1 and T_2 , respectively.

3. Results and discussion

The samples of Ba₄(Nd_{0.7}Sm_{0.3})_{9.33}Ti₁₈O₅₄ (BNST) ceramics with different silver or BaBS content were sintered into dense bodies at different temperatures. The sintering temperature and relative density of each composition are listed in Table 1. The relative densities of sintered samples were plotted as a function of sintering temperatures (shown in Fig. 1). The density of undoped samples saturated at 1250 °C. This was lower than that prepared by the solid-state reaction method or the wet chemical methods, where the sintering temperatures of above 1400 °C or 1350 °C were required [8,13,14], owing to the high sinterability of the nano-powders prepared by the citrate sol–gel process. It is evident that both the silver metal and BaBS glass can improve the sinterability of the BNST ceramics. For the silver-doped samples, the sintering tempera-

Table 1
The sintering temperatures, densities and microwave properties of the modified Ba₄(Nd_{0.7}Sm_{0.3})_{9.33}Ti₁₈O₅₄ ceramics

Dopants	Sintering temperature (°C)	Relative density (%)	Dielectric constant	<i>f</i> (GHz)	<i>Q</i> × <i>f</i> (GHz)	τ_f (ppm/°C)
Undoped	1250	95.4	81.2	5.266	10,800	+9.0
0.5 wt% Ag	1150	95.5	81.1	4.606	11,000	+3.0
1 wt% Ag	1100	94.7	81.2	4.841	11,000	+1.4
2 wt% Ag	1150	94.4	84.0	4.983	6,400	+13
3 wt% Ag	1200	94.9	90.2	5.291	4,000	+19
1 wt% BaBS	1100	93.2	76.6	5.774	8,200	+13
2 wt% BaBS	1000	94.1	76.3	6.261	8,300	+18
4 wt% BaBS	1000	93.6	75.5	6.249	7,500	+25

ture decreased from 1250 °C to 1100 °C with the addition of silver before 1 wt%, and then slightly increased to 1200 °C with further increasing silver addition. For the BaBS-doped samples, the sintering temperature decreased from 1250 °C to 1000 °C with BaBS addition, and it did not get affected by the addition of BaBS from 2 wt% to 4 wt%. Although similar results obtained by these two types of doping, the mechanism for lowering sintering temperature might be different. For the silver doping case, the main possible reason is the formation of space charges at the Ag/BNST interface, leading to increased oxygen vacancies enhancing grain boundary diffusion. The sintering aids effects might be inhibited due to the weak wettability of silver on BNST [14]. For the other BaBS doping case, the decrease in sintering temperature is due to the liquid phase sintering, which usually occurs in the glass-doped ceramic systems [16,17]. The different mechanisms for sintering behavior are responsible for the different microstructure evolutions as discussed in the following.

The XRD analysis was carried out on the samples with maximum relative densities and the results are shown in Fig. 2. The recorded XRD data for all samples can be indexed according to the tungstenbronze-type structure (JCPDS No. 44-0061). For the 1 wt% and 3 wt% Ag-doped samples, no apparent secondary phase was observed. The secondary phase is not found in any BaBS-doped samples either; because of the BaBS materials are least susceptible to crystallization [18]. These results indicate that both silver and BaBS additions did not affect the crystallization of the tungstenbronze-type phase. Hence, the promised dielectric properties of tungstenbronze-type ceramics are possible and expected.

Figs. 3 and 4 demonstrate the microstructure of the Ag- and BaBS-doped BNST ceramics with different doping content, respectively. Uniform well-densified ceramics with almost no porosity were observed for all samples. It is noticeable that the microstructure of the silver- and BaBS-doped ceramics has different morphology. The silver-doped samples exhibit approximately isoaxial grains with the ultrafine grains of about 200–300 nm. Only a few columnar grains were observed

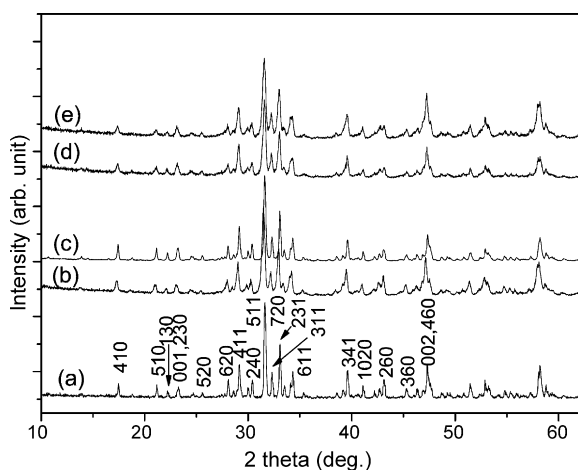


Fig. 2. XRD patterns of the modified BNST ceramics with maximum densities: (a) undoped; (b) 1 wt% Ag-doped; (c) 3 wt% Ag-doped; (d) 2 wt% BaBS-doped; (e) 4 wt% BaBS-doped.

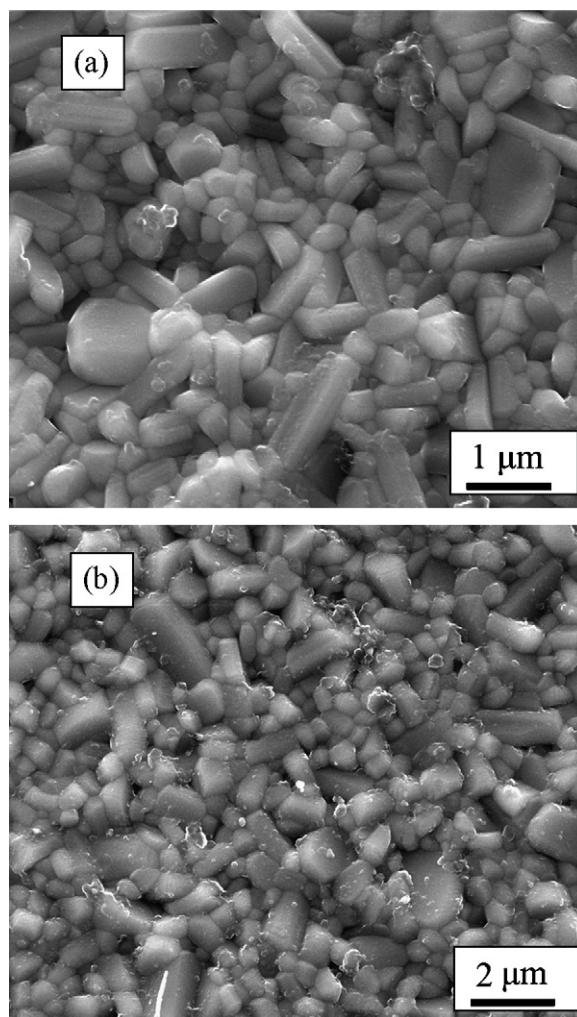


Fig. 3. SEM micrographs of Ag-doped BNST ceramics: (a) 1 wt%, 1150 °C and (b) 3 wt%, 1200 °C.

and their ratio of length to diameter (L/D) is rather small. These are much different from those reported in previous literatures [6,13,19–21], where the columnar grains with large grain size were often observed. While for the other case, the BaBS-doped samples have the typical columnar grains morphology. A tendency of the increase in L/D is also apparently observed with increasing BaBS content. The different morphology obtained here was thought to be related to the different effects of silver and BaBS glass in the BNST ceramic matrix during the sintering process. As mentioned above, the weak wettability of silver on BNST inhibits the grain boundary diffusion, thus limiting the grain growth [15]. On the contrary, the liquid phase formed due to the BaBS glass additions increases grain boundary diffusion and therefore enhances the grain growth along certain direction.

The dielectric properties at microwave frequencies were measured on the sintered ceramics samples and the results are given in Table 1. The variation of microwave dielectric properties of the doped BNST ceramics with dopant content is illustrated in Fig. 5. The dopants (silver metal or BaBS glass) have apparently different effects on the variation of microwave

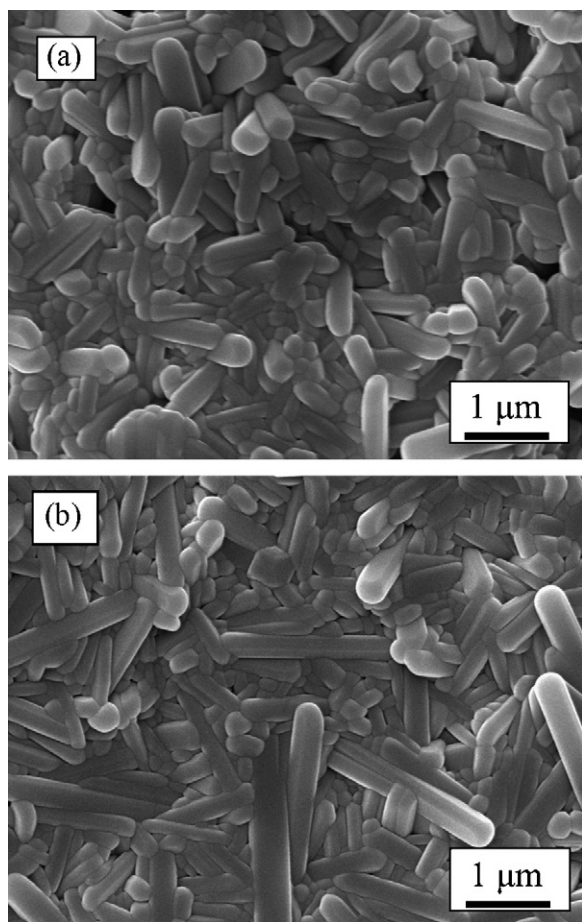


Fig. 4. SEM micrographs of BaBS-doped BNST ceramics: (a) 2 wt%, 1000 °C and (b) 4 wt%, 1000 °C.

dielectric properties. The dielectric constant did not change with less than 1 wt% silver content, and abruptly increased from ~ 81 to ~ 91 with increasing silver content from 1 wt% to 3 wt%. This trend can be explained by the percolation theory. When silver content is >1 wt%, the ceramics can be viewed as insulator-conductor composites. The dielectric constant will increase with silver conductor content in the neighborhood of the percolation threshold. This mechanism also has a strong effect on the dielectric loss and cause the decrease of $Q \times f$ values, as shown in the following. On the contrary, the dielectric constant of the BaBS-doped samples slightly decreased from ~ 81 to ~ 75 with increasing BaBS content up to 4 wt%, since the dielectric constant of BaBS glass is much smaller than that of BNST ceramics [18]. This can be easily explained by the mixing rule of dielectrics as expressed by the Maxwell–Wagner’s equation. The $Q \times f$ values decreased with increasing dopant content from 1 wt% to 4 wt% for both systems. The variation of $Q \times f$ values with dopant content can be explained by similar mechanisms as those for their dielectric constant variation discussed above. Especially, the sample with less than 1 wt% silver additions yielded a highest $Q \times f$ value of about 11,000 GHz, which was comparable to that prepared by the solid-state reaction method. Bearing in mind that the silver-doped system had an average grain size of 250 nm, it was worthy to note that the $Q \times f$ values were not degraded in the

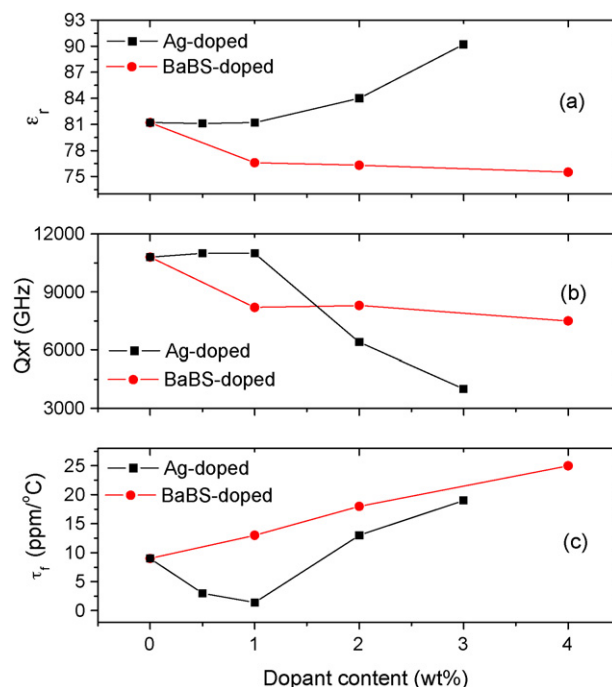


Fig. 5. Variations of microwave dielectric properties with dopant content (wt%) for Ag- or BaBS-doped BNST ceramics with maximum densities: (a) dielectric constant, ϵ_r ; (b) quality factor, $Q \times f$; (c) temperature coefficient of resonant frequency, τ_f .

ultrafine-grain system. It implied that the microwave dielectric loss was not markedly increased with decrease of grain size down to 250 nm, although the reduction in grain size might increase the grain boundary volume in the ceramic matrix. One of the possible explanations might be due to the formation of near isoaxial grains, where the porosity was decreased compared with that among the columnar grains. The τ_f value was decreased from 9 ppm/°C to ~ 2 ppm/°C with silver content from 0 to 1 wt%, whereas it significantly increased up to 19 ppm/°C with 3 wt% silver content. Unlike the τ_f variation in silver-doped samples, the τ_f value gradually increased to 25 ppm/°C with increasing BaBS additions. The abrupt increase of τ_f value in the silver-doped system was attributed to the increase of the corresponding dielectric constant due to the percolation effect.

4. Conclusions

Tungstenbronze-type like $\text{Ba}_4(\text{Nd}_{0.7}\text{Sm}_{0.3})_{9.33}\text{Ti}_{18}\text{O}_{54}$ microwave ceramics doped with 0–3 wt% silver particles were prepared by a citrate sol–gel method. The $\text{BaO-B}_2\text{O}_3\text{-SiO}_2$ glass was also added into the sol–gel derived BNST ceramic powders as sintering aids. The undoped samples can be sintered at 1250 °C, while the Ag- and BaBS-doped samples can be sintered into dense ceramics at 1150 °C and 1000 °C with dopant content of 1 wt% and 2 wt%, respectively. Near isoaxial grains with about 250 nm was obtained for the silver-doped samples, and typical columnar grains was observed for the BaBS-doped counterparts. The different microstructure was related to the different sintering behaviors during the sintering

process. The former dammed the grain boundary diffusion due to the weak wettability of silver particles on BNST matrix. The latter enhanced the grain growth owing to the formation of liquid phase. For the silver-doped samples, the dielectric constant and dielectric loss are not affected when <1 wt% silver content, while with further increase of silver content, both dielectric constant and dielectric loss increased due to the percolation effect. A bend of the τ_f value also occurred at 1 wt% silver content. For the BaBS-doped ones, both dielectric constant and $Q \times f$ decreased, whereas the τ_f value increased with increasing BaBS content.

Acknowledgements

This work was supported by the Ministry of Science and Technology of China through 973-Project under 2002CB613307, the Natural Science Foundation of China (Grant Nos. 50672043, 50621201 and 50632030).

References

- [1] W. Wersing, Microwave ceramics for resonators and filters, *Curr. Opin. Solid State Mater. Sci.* 1 (1996) 715–731.
- [2] T. Negas, P.K. Davies, Influence of chemistry and processing on the electrical properties of $\text{Ba}_{6-3x}\text{Ln}_{8+2x}\text{Ti}_{18}\text{O}_{54}$ solid solutions, *Ceram. Trans.* 53 (1996) 179–196.
- [3] R. Ubbelohde, I.M. Reaney, W.E. Lee, Microwave dielectric solid-solution phase in system $\text{BaO-Ln}_2\text{O}_3\text{-TiO}$ (Ln = lanthanide cation), *Int. Mater. Rev.* 43 (5) (1998) 205–219.
- [4] M. Valant, D. Suvorov, C.J. Rawn, Intrinsic reasons for variations in dielectric properties of $\text{Ba}_{6-3x}\text{R}_{8+2x}\text{Ti}_{18}\text{O}_{54}$ (R = La–Gd) solid solutions, *Japanese J. Appl. Phys.* 38 (1999) 2820–2826.
- [5] H. Ohsato, Science of tungstenbronze-type like $\text{Ba}_{6-3x}\text{R}_{8+2x}\text{Ti}_{18}\text{O}_{54}$ (R = rare earth) microwave dielectric solid solutions, *J. Eur. Ceram. Soc.* 21 (2001) 2703B.
- [6] X.M. Chen, Y. Li, A- and B-site co-substituted $\text{Ba}_{6-3x}\text{Sm}_{8+2x}\text{Ti}_{18}\text{O}_{54}$ microwave dielectric ceramics, *J. Am. Ceram. Soc.* 85 (3) (2002) 579–584.
- [7] H. Ohsato, H. Kato, M. Mizuta, S. Nishigaki, T. Okuda, Microwave dielectric properties of the $\text{Ba}_{6-3x}(\text{Sm}_{1-y}\text{R}_y)_{8+2x}\text{Ti}_{18}\text{O}_{54}$ (R = Nd and La) solid solution with zero temperature coefficient of the resonant frequency, *Japanese J. Appl. Phys.* 34 (9B) (1995) 5413–5417.
- [8] H. Ohsato, M. Imaeda, The quality factor of the microwave dielectric materials based on the crystal structure- as an example: the $\text{Ba}_{6-3x}\text{R}_{8+2x}\text{Ti}_{18}\text{O}_{54}$ (R = rare earth) solid solutions, *Mater. Chem. Phys.* 79 (2003) 208–212.
- [9] K. Wada, K. Kakimoto, H. Ohsato, Grain-orientation control and microwave dielectric properties of $\text{Ba}_4\text{Sm}_{9.33}\text{Ti}_{18}\text{O}_{54}$ ceramics, *Japanese J. Appl. Phys.* 42 (2003) 6149–6153.
- [10] B.W. Hakki, P.D. Coleman, A dielectric resonator method of measuring inductive capacitors in the millimeter range, *IRE Trans. Microwave Theory Tech. MMT-8* (1960) 402–410.
- [11] W.E. Courtney, Analysis and evaluation of a method of measuring the complex permittivity and permeability of microwave insulators, *IEEE Trans. Microwave Theory Tech. MMT-18* (1970) 476–485.
- [12] W. Wersing, High Frequency Ceramic Dielectrics and Their Applications for Microwave Components, *Electronic Ceramics*, New York, 1991, pp. 67–119.
- [13] Y.B. Xu, G.H. Huang, Y.Y. He, Sol-gel preparation of $\text{Ba}_{6-3x}\text{Sm}_{8+2x}\text{Ti}_{18}\text{O}_{54}$ microwave dielectric ceramics, *Ceram. Int.* 31 (1) (2005) 21–25.
- [14] P. Setasuwon, R. Freer, F. Azough, C. Leach, $(\text{Ba}_{1-y}\text{Pb}_y)_{3.75}\text{Nd}_{9.5}\text{Ti}_{18}\text{O}_{54}$ and $(\text{Ba}_{1-y}\text{Sr}_y)_{3.75}\text{Nd}_{9.5}\text{Ti}_{18}\text{O}_{54}$ microwave dielectric ceramics: effect of Pb and Sr substitution on dielectric properties, *Br. Ceram. Trans.* 101 (2002) 237–241.
- [15] R.Z. Chen, X.H. Wang, Z.L. Gui, L.T. Li, Effect of silver addition on the dielectric properties of barium titanate-based X7R ceramics, *J. Am. Ceram. Soc.* 86 (2003) 1022–1024.
- [16] H.T. Kim, S.H. Kim, S. Nahm, J.D. Byun, Low-temperature sintering and microwave dielectric properties of zinc metatitanate–rutile mixtures using boron, *J. Am. Ceram. Soc.* 82 (11) (1999) 3043.
- [17] S.H. Wee, D.W. Kim, S.I. Yoo, Microwave dielectric properties of low-fired ZnNb_2O_6 ceramics with BiVO_4 addition, *J. Am. Ceram. Soc.* 87 (5) (2004) 871–874.
- [18] C.S. Chen, C.C. Chou, W.J. Shih, K.S. Liu, C.S. Chen, I.N. Lin, Microwave dielectric properties of glass–ceramic composites for low temperature co-firable ceramics, *Mater. Chem. Phys.* 79 (2003) 129–134.
- [19] A. Silva, F. Azough, R. Freer, C. Leach, Microwave dielectric ceramics in the system $\text{BaO-Li}_2\text{O-Nd}_2\text{O}_3\text{-TiO}_2$, *J. Eur. Ceram. Soc.* 20 (2000) 2727–2734.
- [20] S.F. Wang, Y.F. Hsu, Y.R. Wang, L.T. Chenga, Y.C. Hsua, J.P. Chu, C.Y. Huang, Densification, microstructural evolution and dielectric properties of $\text{Ba}_{6-3x}(\text{Sm}_{1-y}\text{Nd}_y)_{8+2x}\text{Ti}_{18}\text{O}_{54}$ microwave ceramics, *J. Eur. Ceram. Soc.* 26 (2006) 1629–1635.
- [21] J.M. Wu, M.C. Chang, Reaction sequence and effects of calcination and sintering on microwave properties of $(\text{Ba,Sr})\text{O-Sm}_2\text{O}_3\text{-TiO}_2$ ceramics, *J. Am. Ceram. Soc.* 73 (1990) 1599.